Research on the Utility of Anti-smoke Air Curtain in Flue Gas Control on Luxury Cruise Ships

Saili Yi*, Bin Huang
School of Urban Construction and Safety Engineering, Shanghai Institute of Technology, Shanghai, China
**Corresponding Author*

Abstract: While sprinkler systems are internationally recognized as the most effective indoor fire protection measures, they still exhibit limitations in addressing specific fire scenarios such as those occurring in cruise ships' high-ceiling spaces. These limitations primarily manifest as smoke deposition caused by thermal buoyancy failure and blind zones in water system coverage. To overcome these challenges, this study proposes a non-water-based supplementary solution centered on smoke barriers, with a focus on analyzing how the outlet jet velocity and angle of composite material-made smoke barriers affect their smoke-blocking effectiveness. The results demonstrate that smoke barriers, as an auxiliary firefighting measure, combine excellent thermal insulation and smoke-blocking performance, effectively enhancing fire protection capabilities in such specialized spaces.

Keywords: Luxury Cruise Ship; Building Information Modeling (BIM); Fire Simulation; FDS; Smoke Curtain; Smoke Control

1. Introduction

The cruise tourism industry has a long supply chain and spans a wide range of sectors, playing a significant role in driving the socio-economic development of a nation [1]. However, frequent ship fires pose a serious threat to the safety of crew members' lives and property. Common locations for fires on cruise ships are shown in Table 1. Jia & lu [2] verified that sprinkler systems can effectively suppress the development of cruise ship fires. However, ship compartments consist of multi-layered enclosed spaces, narrow passages, and complex compartments. During a fire, high-temperature smoke and toxic gases such as carbon monoxide rapidly accumulate, causing visibility to plummet and restricting evacuation routes; Steel ship hulls have high thermal conductivity, and heat rapidly conducts through bulkheads and decks, creating a “thermal bridge effect” that ignites adjacent combustible materials; stairwells and shafts connect all deck levels, and fire smoke is driven upward by the “chimney effect,” easily developing into multi-level fires. Without altering the ship's original structure, smoke curtains made of composite materials can form a flexible barrier to prevent smoke from spreading from the fire area to other areas. This study involves coating the metal substrate of the smoke curtain with nano-SiO_2 silicon-based composite materials to enhance surface thermal reflectivity, while also being easy to install and requiring no modification to the smoke curtain's main structure.

This paper conducts a fire simulation of the “Golden No. 5” luxury cruise ship along the atrium shops on the Yangtze River using FDS. It introduces composite material smoke curtains as a new fire protection measure to safeguard cruise ship safety. The study focuses on analyzing the impact of different jet velocities, angles, and combinations with sprinkler systems on smoke blocking efficiency and thermal insulation efficiency. It explores the feasibility of smoke curtains in addressing fire protection challenges in the high-ceilinged spaces of ships where sprinkler installation is inconvenient. to enhance fire prevention and control during the design, construction, and operation of cruise ships.

Table 1. Common Fire Locations on Cruise Ships

Common fire locations on cruise ships Fire location	cockpit	Passenger cabin	Stores	Dining Room	Theater	Bars	Boardroom	Deck	Atrium	Bookstore	Distribution room	Other
Sprinkler Applicable	Applicable							Not applicable				

2. Domestic and Overseas Research Status

The air curtain technology was first applied by Soviet scholars in mines to improve harsh working conditions. In the early 1980s, Japanese researchers pioneered its application in high-rise building smoke control systems through experimental studies, achieving remarkable results [3]. With

advancements in computing power and fluid mechanics theories, air curtains have been validated through numerical simulations, theoretical analyses, and full-scale experiments, establishing their effectiveness as a novel flexible smoke barrier technology. Early foundational research: Hayes& Stoecker [4] demonstrated through experimental and theoretical analysis that the minimum bending modulus required for stable air curtain operation correlates with relative length and initial jet angle, with corresponding relationship diagrams developed. British scholars Ge & Tassou [5] established a finite difference method-based computational model for refrigeration cabinet air curtain optimization. In 2007, Hu et al. [6] confirmed air curtains 'efficacy in containing smoke and carbon monoxide (CO) spread during long corridor fires. By 2010, Yang et al. [7] conducted comparative studies using experimental data and FDS software simulations, demonstrating air curtains' superiority over natural ventilation walls, mechanical exhaust systems, and conventional smoke barriers in natural ventilation corridors. In 2012, Chun & Li [8]'s numerical simulations showed air curtains could effectively control pollutant dispersion in hospitals without compromising patient comfort. Portuguese scholar Goncalves et al. [9] evaluated the partition efficiency of air curtains installed at different positions in cold storage facilities (indoor, outdoor, and both sides of doors). The study found that the downward-airflow air curtain installed outdoors achieved over 70% efficiency, while the side-airflow type only reached 55%. Although circulating air curtains demonstrated higher efficiency, their limited application was constrained by complex installation and high maintenance costs. In 2014, Spanish researcher Tomas et al. [10] 's research further indicated that installing air curtains at cold storage doors could reduce heat transfer by up to 80% compared to traditional physical partition methods. At the Naval University of Engineering, Zhong et al. [11-12] proposed and validated a method to enhance air curtain smoke-blocking performance through theoretical analysis and numerical simulation: utilizing two opposing staggered jets to intensify the pseudo-ordering of turbulent motion, with experimental verification confirming its feasibility. In 2017, Luo et al. [13] conducted 1:12 scale experiments and FDS validation to study air curtain smoke-blocking effects at stairwell entrances, revealing that ventilation outlet positioning significantly impacts performance (reverse arrangement between air curtains and vents yields better results) and that jet velocity isn't always optimal—dynamic adjustments during fire progression are required to maintain maximum effectiveness. That same year, Zhang et al. [14] discovered in high-rise building fire research that increasing air curtain flow enhances smoke-blocking performance, but the resulting pressure differential from evacuation weakens its effectiveness. In 2020, Razeghi et al. [15] conducted simulation studies on smoke-blocking characteristics when air curtains and mechanical smoke exhaust systems work synergistically, examining the combined effects of different air curtain jet velocities, angles, and exhaust volumes. Zhang et al. [16] proposes a system for separating smoke on subway platforms using a combination of external air supply platform air curtains, stair (or escalator) air curtains, and a mechanical smoke exhaust system. Yu et al. [17] proposes an adaptive intelligent smoke control method combining PID (Proportional Integral Derivative) system with a traditional air curtain. Li et al. [18] foucus on a study on the smoke sealing efficiency of air curtain and maximum ceiling temperature rise under longitudinal ventilation in bifurcated tunnel. Lu et al. [19] investigated the influence of the HRR, jet velocity, longitudinal velocity, and bifurcation angle on the smoke sealing efficiency of the air curtain by numerical simulations. In other fields, research on material combustion behavior under oxygen-rich environments has provided support for related safety applications. A study by Paulo Cesar Franca da Camara et al. [20] (2025) demonstrated that introducing cellulose nanocrystals (CNCs) into the PAM-PEI/glycerol gel system significantly suppresses dehydration shrinkage and extends the linear viscoelastic region (with a loss factor reduced below 0.1). By leveraging CNC's thermal insulation properties, the system effectively mitigates pressure buildup in annular spaces (APB), providing innovative insights for high-temperature sealing and refractory material design.

In recent years, significant advancements have been achieved in the application of nanomaterials for fire protection. Shi et al. [21-22] investigated the properties of nano-SiO_2 modified acrylic resin coatings, confirming their exceptional thermal stability and flame-retardant characteristics. Gao et al. [23] validated the synergistic flame-retardant mechanism between nano-SiO_2 and fire retardants, demonstrating substantial enhancement in the material's Limiting Oxygen Index (LOI) and char residue yield. Liang [24] applied nano-SiO_2 composite flame-retardant materials to marine fire

protection design, proving their effectiveness in blocking the 'thermal bridging effect' in steel structures. These studies collectively establish the theoretical foundation and technical support for implementing nano-SiO_2/zinc borate composite flame retardants in smoke-blocking curtain wall systems.

3. Fire Scenario Analysis and Design

3.1 Fire Scenario Analysis

Fire load design needs to be considered according to the actual situation. He et al. [25] A practical investigation of the fire loads of 145 clothing stores confirms that there is a large gap in fire loads between different areas. Cheng [26] fitted the fire load data of large shopping malls and found that it approximately obeys a normal distribution, and obtained the average value of fire density of shopping malls as 543 MJ/m2. Therefore, the silk store fire load in this chapter is set to 0.5 MW, and a rapid fire is used to maximize the fire power at 103.2 s. The simulation time is too long. The simulation time is too long to ignore the effect of settling smoke on the atrium of the first floor, and in order to develop the fire as much as possible, the simulation time is set to 250 s. The atmospheric pressure, ambient wind speed, and temperature are set to 101.325 kPa, 0 m/s, and 20 °C, respectively.

According to the formula $D^*=\left(\frac{Q}{\rho_\infty C_p T_\infty \sqrt{g}}\right)^{\frac{2}{5}}$, the characteristic flame diameter D* is calculated to be 0.729 m. By taking the grid size as 1/4-1/16 of the characteristic flame diameter D* for quantitative meshing, the grid size near the fire source is calculated to be 0.18 m at most. The grid size of the whole model is 16 m × 16 m × 3 m. After mesh sensitivity analysis, the grid size is set to be 0.16 m × 0.16 m × 0.15 m. The safety exits of the fire room 1.5 m are set to be 0.15 m. The fire source is set to be 0.15 m. The fire source is set to be 0.16 m. The fire source is set to be 0.16 m. When the temperature of the fire room reaches 180 °C, as detected by the temperature probe at a height of 1.8 m at the safety exit of the fire room, the door of the room is opened. In the store door as well as windows inside and outside, every 0.1 m, set up a group of detection points, a total of 10 groups, each group of detection points had a height of 0.5 m, 1 m, 1.5 m, and 2 m. In the ignition source above the 0.5 m in the 0.3 m × 0.3 m square at equal spacing, respectively, set up nine temperature and oxygen concentration detection points. Meanwhile, temperature, visibility, vector flow rate slices, and heat flow measurements were set up in the middle of the store door, window, and atrium corridor, respectively. A 1.5 m × 0.15 m (the width of the room door is 1.2 m) wind screen one is set up in front of the room door, and a 5 m × 0.2 m wind screen two is set up in front of the window (the farthest distance between the two windows is 4.65 m). The specific parameters of the wind screen are shown in Table 2, and the fire model, probe, and wind screen arrangement are shown in Figure 1.

Table 2. Fan Curtain Parameter Settings

No.	Location of wind curtain	Name of wind curtain	Wind curtain wind speed (m/s)	Air volume (m^3/h)
1	--	None	0	0
2	Doorway	Air curtain 1	5	5940
3		Air curtain 1	10	11880
4		Air curtain 1	15	17820
5	Window	Wind screen 2	5	18000
6		Wind screen 2	10	36000
7		Wind screen 2	15	54000

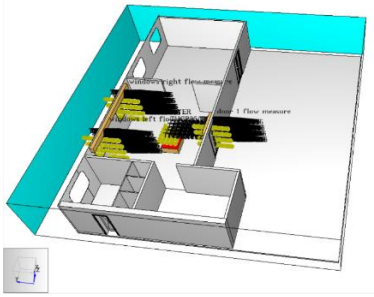

Figure 1. Fire Model and Its Related Equipment Arrangement

3.2 Simulation of Conditions

In order to study the effect of spray and smoke air curtains on fire safety of ships, and to investigate the effects of wind speed and air outlet angle of air curtains under different parameter designs, 12 groups of conditions are set up in this chapter, of which condition 1 is the control group, and the remaining 11 groups are the experimental groups, and the specific programs are shown in Table 3.

3.3 Materials and Design of Smoke Curtains

The outlet vent and deflector components of the fire-smoke air curtain are fabricated from a composite material comprising nano-SiO_2 blended with zinc borate flame retardant, where nano-SiO_2 constitutes 6% by mass. This material exhibits the following characteristics:(1) A Limiting Oxygen Index (LOI) of 30.8% with UL 94 V-0 classification;(2) Structural integrity maintenance for 2 hours at 700°C;(3) Thermal conductivity reduced by >80% compared to conventional

metallic materials;(4) The dense carbon layer is formed through Si-O-P cross-linking structure. This design prevents high-temperature flue gas from causing deformation or failure of the outlet, while avoiding secondary ignition risks caused by thermal conduction in traditional metal materials. It achieves ultra-low thermal conductivity and maintains structural integrity for over 2 hours at 700°C high temperature, effectively blocking heat transfer and flame propagation. This provides a dual protective barrier for ship steel structures.

Table 3. Simulation Scenarios

Research content	conditions	Fire-fighting measures
Impact of wind speed on cruise ship Impact of Wind Curtain Wind Speed on Cruise Ship Safety	condition 1	Wind screen (wind speed 0m/s, angle 0°)
	condition 2	Wind screen (wind speed 2.5m/s, angle 0°)
	condition 3	Wind curtain (wind speed 5m/s, angle 0°)
	condition 4	Wind curtain (wind speed 7.5m/s, angle 0°)
	condition 5	Wind curtain (wind speed 10m/s, angle 0°)
	condition 6	Wind curtain (wind speed 10m/s, angle 0°)
	condition 7	Wind screen (wind speed 15m/s, angle 0°)
Wind curtain angle on cruise Influence on the Safety of Cruise Ships	condition 5	Wind screen (wind speed 10m/s, angle 0°)
	condition 8	Wind screen (wind speed 10m/s, angle 5°)
	condition 9	Wind curtain (wind speed 10m/s, angle 10°)
	condition10	Wind curtain (wind speed 10m/s, angle 15°)

The functionalized coating adopts a gradient composite structure design, with an outer layer of high-density SiC ceramic layer with a thermal conductivity of 14 $W \cdot m^{-1} \cdot K^{-1}$ to withstand direct impact from open flames; the inner layer consists of nano-SiO_2 composite phase-change materials, which delay heat transfer through melting and heat absorption, forming a synergistic protective system of "high-strength thermal insulation-heat absorption buffering" from the outer to the inner layers. This structure alleviates thermal stress between the coating and the ship's steel substrate through compositional gradient changes, preventing interface peeling caused by differences in thermal expansion coefficients. Additionally, the porous structure of the inner layer's nano-SiO_2 significantly reduces thermal conductivity, effectively blocking the "thermal bridge effect" in steel structures. Water-based slurry is applied via high-pressure airless spraying, suitable for ship curved surfaces, with a single coat thickness of 80–100 μm, and two coats are sufficient to meet fireproofing requirements. During construction, only simple sandblasting rust removal (Sa2.5 grade) is required, without the need to dismantle equipment or perform complex substrate pretreatment. The slurry is stably conveyed via a dual-channel peristaltic pump and uniformly sprayed by an atomizing nozzle, with curing completed within 24 hours.

4. Research on the Effect of Wind Speed on the Smoke Barrier Effect of Air Curtains

4.1 Effect of Different Smoke Barrier Air Curtain Wind Speeds on Combustion Parameters

As shown in Figure 2, the temperatures above the fire source are ranked in descending order as follows: Condition 3 > Condition 2 > Condition 1 > Condition 4 > Condition 5 > Condition 6 > Condition 7. When the air curtain wind speed is low, the temperature above the fire source is positively correlated with the wind speed; when the air curtain wind speed is high (≥7.5 m/s), the temperature above the fire source is negatively correlated with the wind speed. When the air curtain wind speed increases from 5 m/s to 7.5 m/s, the temperature above the fire source decreases sharply by approximately two-thirds. It can be observed that the temperature above the fire source is highly sensitive to the air curtain wind speed. Therefore, when applying air curtains in ship fire protection design, it is necessary to conduct detailed research on the wind speed based on actual conditions.

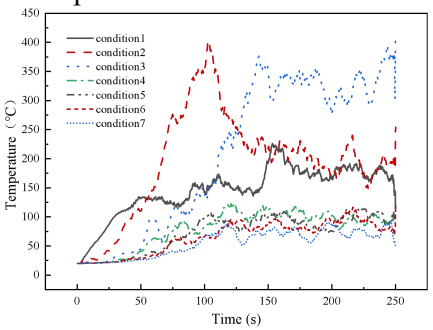

Figure 2. Temperature Curve above the Ignition Source (1.8m from the Ground)

4.2 Effects of Different Smoke Curtain Air Velocity on Fire Environment Parameters

4.2.1 Temperature

During the stable combustion stage (200 s-250 s), the temperature change near the door at a height of 2 m is shown in Figure 3, and it can be found that the temperature in front of the door is higher than that behind the door regardless of whether the air curtain is open or not. This is due to the fact that the closer the fire source, the stronger the thermal radiation effect, and the chamber wall has better thermal insulation. The temperature after the wind screen and the room temperature are not much different, reflecting the excellent thermal insulation effect of the wind screen. When the wind speed of the air curtain is not less than 10 m/s, the exit temperature of the fire room is lower than 60 ℃, which can be used as a safety exit for evacuation. In order to quantify the effect of fire protection measures on reducing the temperature of the fire scene, the temperature change rate of 1 m in front of and behind the door during the stable combustion phase is defined as the insulation efficiency, and the insulation efficiency is used to illustrate the thermal insulation effect of the smoke curtains, which is shown in Equation (1). The calculated thermal insulation efficiency in order of magnitude is as follows: condition 3>condition 2>condition 1>condition 4>condition 5=condition 6>condition 7. The thermal insulation efficiency of the air curtain is highest at a wind speed of 5 m/s, reaching 99.36 %. In addition, there is not much difference in T2as well as room temperature between conditions 1-7, and the thermal insulation efficiency is mainly related to the size of T1.

$$\eta_T = \frac{T_1 - T_2}{T_1 - T_0} \tag{1}$$

Where: η_T is the insulation efficiency; T_0 is the room temperature; T_1 is the flue gas temperature before the air curtain; T_2 is the flue gas temperature after the air curtain.

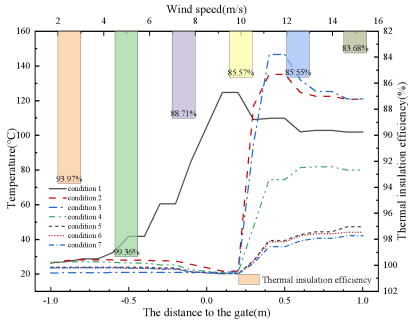

Figure 3. Stable Combustion Stage, Temperature Change Curve Near the Door and Thermal Insulation Efficiency Diagram

4.2.2 Visibility

It is generally recognized that visibility below 10 m in tall spaces will have a greater impact on pedestrian evacuation speed. In the 3D view of the FDS fire simulation results, the equivalent surfaces with visibility of 5 m and 10 m are highlighted, in which the dark purple area has visibility of 5 m and the light purple area has visibility of 10 m, and the 3D distribution of the equivalent surfaces with visibility of 5 m and 10 m is obtained in Figure 4. In condition one and condition 2, the visibility in the top area of the atrium near the fire room is less than 10 m, while the visibility in other areas is more than 10 m. Most of the visibility in the atrium area in conditions 3-7 does not meet the safety requirements. It can be found that the wind speed of the wind screen is too large (≥5 m/s), which is not conducive to improving the visibility of the atrium.

4.2.3 CO concentration

From Figure 5, it can be found that when the wind speed of the wind screen increased from 0 m/s to 15 m/s, the CO concentration in the fire compartment at 250 s showed a trend of increasing and then decreasing, of which the wind speed of the wind screen was the most serious when the wind speed was 7.5 m/s, and the threshold surface of the CO concentration was in the highest position when the wind speed was 15 m/s.

4.3 Effects of Different Smoke Curtain Air Speeds on Smoke Movement

4.3.1 Cloud diagram of smoke movement

As can be seen from Figure 6, the wind screen affects the direction of smoke propagation. Under no air curtain conditions, fire smoke spreads around almost the same speed, and the air curtain increases the smoke spread to the right, which is greater than the speed of spread to the left (parallel to the direction of the air curtain). At 50 s, the smoke in the fitting room in the lower left corner of the air curtain condition, which was connected to the fire room, was much lower than that in the room. At 90 s, the concentration of smoke in the fitting room with high wind speed (≥10 m/s) is similar to that in condition 1 at 50 s, indicating that the wind screen is effective in blocking the spread of smoke.

4.3.2 Smoke blocking efficiency

Using Origin's mathematical analysis function to integrate the heat flux curve of the detection point to get the heat flux, and comparing it with the control group to get the smoke blocking efficiency of each firefighting measure, the specific formula is shown in Equation 2. From Figure 7, we can get the smoke blocking efficiency of each place according to the size of the order: (1) The smoke blocking efficiency at the door is as follows: condition 3>condition

2>condition 5>condition 4>condition 6>condition 7.
(2) At the left window, the order of smoke blocking efficiency is as follows: condition 4 > condition 6 > condition 7, condition 5 > condition 3 > condition 2.
(3) At the right window, the order of smoke blocking efficiency is as follows: condition 7 > condition 6 > condition 5 > condition 4 > condition 3 > condition 2.

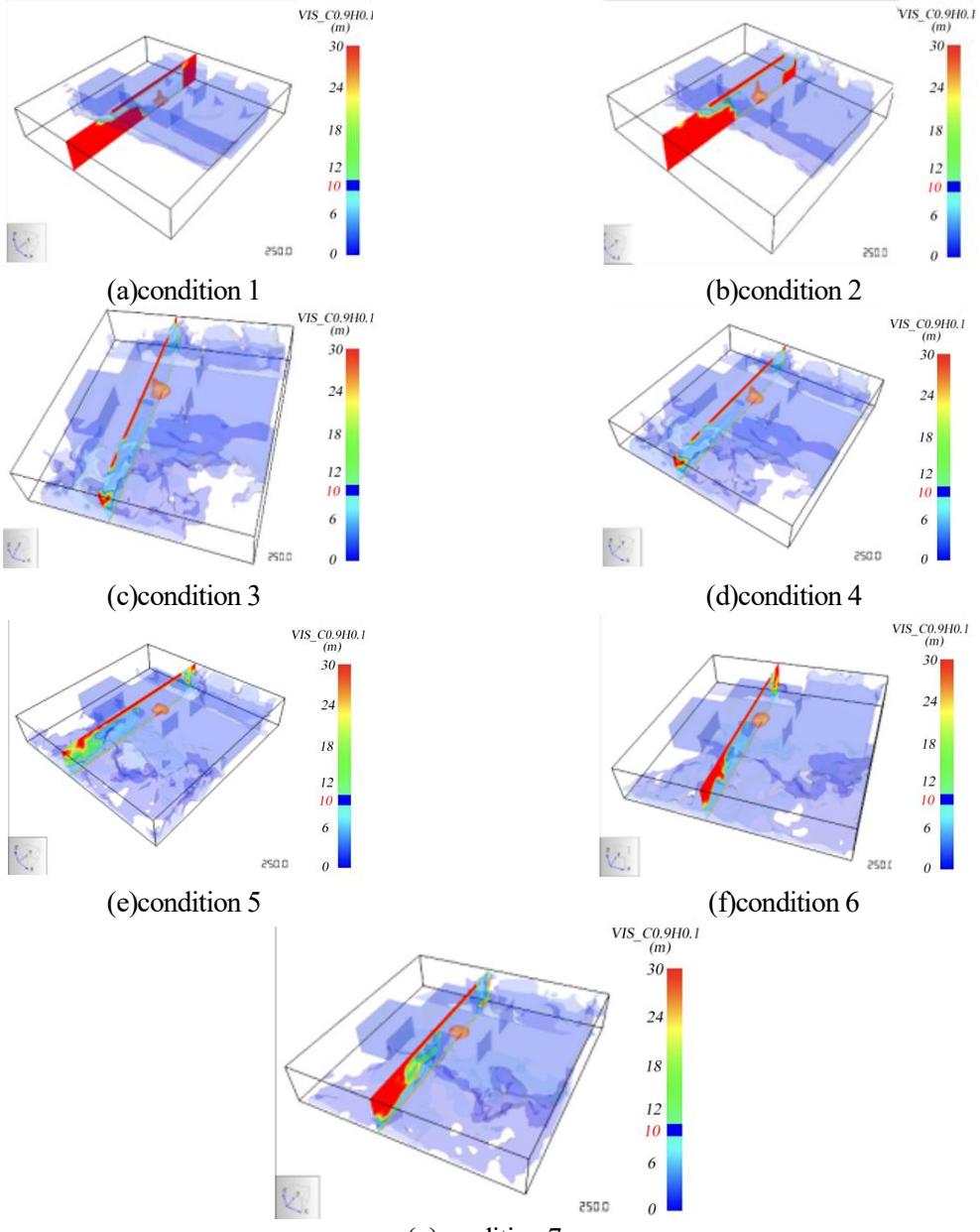

(a)condition 1 (b)condition 2

(c)condition 3 (d)condition 4

(e)condition 5 (f)condition 6

(g)condition 7

Figure 4. 250s, Visibility 5m and 10m Isosurface 3D Cloud Distribution Map

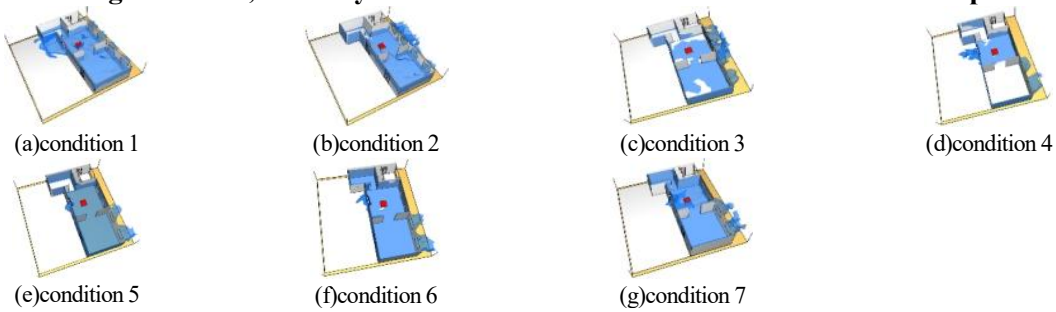

(a)condition 1 (b)condition 2 (c)condition 3 (d)condition 4

(e)condition 5 (f)condition 6 (g)condition 7

Figure 5. 250s, the 500ppmCO Concentration is Equivalent to the Surface Cloud, from Left to Right, the Conditions 1-7

(a) Top view of the smoke diffusion distribution at 20 s, from left to right for conditions 1-7.

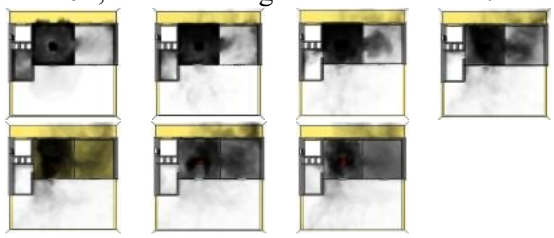

(b)Top view of the smoke diffusion distribution at 50s, from left to right conditions 1-7

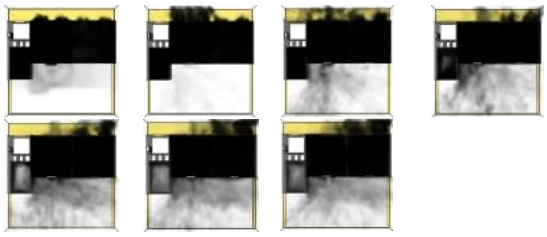

(c) Top view of smoke spread distribution at 90s, from left to right for conditions 1-7

Figure 6. Flue Gas Spread

From Figure 7, it can be found that the smoke blocking efficiency is related to the wind speed of the wind screen as well as the position, which is consistent with the research of other scholars. When the wind speed of the wind screen is lower than 7.5 m/s, both of the wind screen at the door and window can play a positive role in blocking the flow of smoke; when the wind speed is not lower than 7.5 m/s, the wind screen at the door accelerates the diffusion of smoke to the outside, but the role of the wind screen at the window on the blocking of smoke increases with the increase of wind speed.

$$\eta = \frac{l_1 - l_2}{l_1} \times 100\% \tag{2}$$

Where: l_1 indicates the heat flux through the cross-section when the air curtain is opened; l_2 the heat flux through the cross-section after the air curtain is opened; η the smoke-blocking efficiency of the smoke-proof air curtain.

5. The Effect of Different Smoke Curtain Air Outlet Angle on the Smoke Barrier Effect

5.1 Effect of Different Air Curtain Outlet Angles on Combustion Parameters

From Figure 8, we can get the temperature above the fire source in the first 220 s according to the size of the order of: condition 5>condition 9=condition 10>condition 8. The angle of the air curtain is used to reduce the growth of the temperature above the fire source in the early period, to slow down the role of the fire. Increase the air curtain angle of 5 ° relative to other kinds of conditions, the cooling effect is slightly better, but 220 s after the condition 8 temperature from 50 ℃ began to climb abnormally to 150 ℃. It can be found that increasing the angle of the air curtain can play a role in reducing the temperature above the fire source, but we need to pay attention to its impact on the later development of the fire.

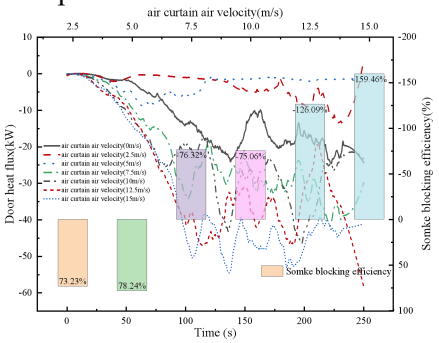

(a) Heat flux and smoke blocking efficiency of doors and windows

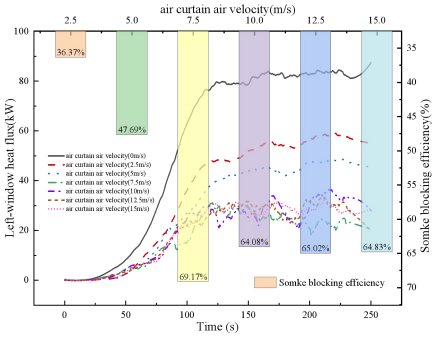

(b) Plot of heat flux and smoke blocking efficiency for left window

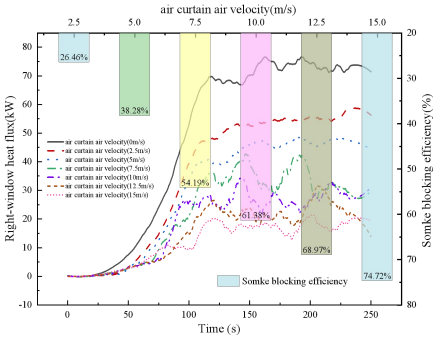

(c) Heat flux and smoke blocking efficiency of the right window.

Figure 7. Heat Flow and Smoke Barrier Efficiency of Doors and Windows with Different Air Curtains, Wind Speeds

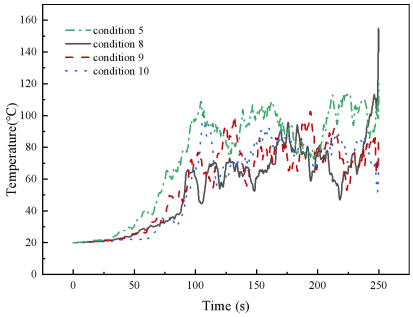

Figure 8. Temperature Change Curve above the Ignition Source (1.8m from the Ground)

5.2 Influence of Different Air Outlet Angles of Smoke Curtain on Fire Environment Parameters

5.2.1 Temperature

From Figure 9, it can be seen that when the air velocity of smoke-proof air curtain is 10 m/s, increasing the angle of smoke-proof air curtain 5° and 10° can reduce the temperature in front of the door. However, the temperatures before and after the safety exit with an air curtain angle of 15° are higher than those in condition 5. This may be because the fire room is small, and a larger angle of the air curtain may result in a larger white area between the exit and the air curtain, and the high-speed flow field near the air curtain wraps the hot smoke through the door and generates thermal convection and thermal radiation, resulting in a serious increase in temperature after the air curtain.

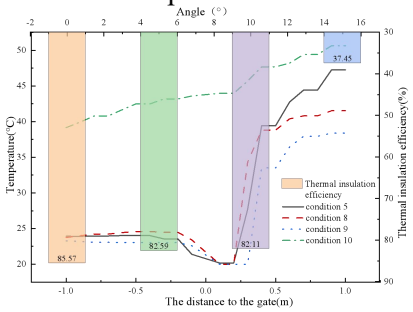

Figure 9. Temperature Change Curve of Stable Combustion Stage at 2m Height

5.2.2 Visibility

As can be seen from Figure 10, The visibility performance of different wind screen angles at 250 s is different in different areas. The lower visibility of the cruise ship facade is different in different locations, with condition 5 occurring below the window, condition 8 and condition 9 occurring at the upper window, and condition 10 not showing any warning for the visibility of the cruise ship facade. Poor atrium visibility in conditions 5 and 8 can have an impact on evacuation. The human eye feature height visibility for condition 9 is almost out of safety. Work condition 10 atrium visibility is so low that passengers can only escape at a slow speed.

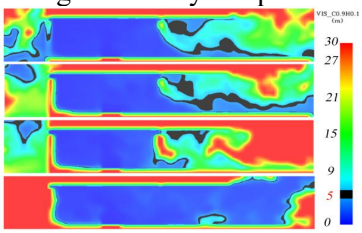

Figure 10. 250s, Visibility Slice Plot, from Top to Bottom, Conditions 5, 8, 9 and 10

5.2.3 CO concentration

From Figure 11, it can be found that the height of the 500 ppm CO concentration contour surface for condition 5 is lower than the height of the fire source (0.5 m), conditions 8 and 10 are close to the height of the fire source, and condition 9 is higher than the height of the fire source. Since the CO concentration value in the area above the 500 ppm CO concentration contour surface is larger, the safety ranking of CO concentration in different wind screen angles can be obtained as follows: condition 9>condition 8 and condition 10>condition 5.

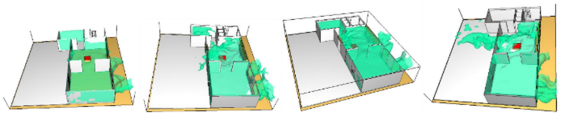

Figure 11. 50s, 500ppmCO Concentration Equivalent Surface Cloud, from Left to Right, Conditions 5, 8, 9 and 10

5.2.4 Smoke-proof wind curtain material

The selection of materials for smoke-proof wind curtains is crucial in determining key performance indicators such as airtightness, heat resistance, and mechanical strength. These materials can be categorized into two primary types based on their composition. Traditional materials often consist of single-layer metal plates, such as galvanized steel or stainless steel sheets. However, these single-layer panels are susceptible to warping and deformation under thermal or mechanical stress, which can make it challenging to maintain a tight seal with building structures during operation, thereby significantly increasing the risk of smoke leakage. The management of splicing seams and installation gaps continues to pose a technical challenge.

This study employs a composite material structure design for smoke-proof wind curtains, utilizing lightweight, high-strength, and low-thermal-conductivity fire-resistant insulation core materials. The inner and outer surfaces are coated with high-strength, weather-resistant, and heat-resistant surface layers, bonded together using high-performance adhesives or physical methods.

Experimental results indicate that the leakage rates

of traditional wind curtains increase exponentially with rising temperatures, (eaching 28.5% at 600°C. In contrast, composite-based wind curtains maintain leakage rates below 4% throughout the process, owing to their flexible sealing and low thermal deformation characteristics. The study reveals that composite material-based wind curtains demonstrate superior high-temperature performance and stability under fire conditions, with no significant deformation observed at elevated temperatures at air outlets. These advantages underscore their enhanced operational reliability compared to conventional metal-based wind curtains.

5.3 Influence of Different Smoke Curtain Outlet Angles on Smoke Movement

5.3.1 Smoke Motion Cloud

Preventing the spread of smoke from the burning compartment to other areas is one of the important performance roles of the air curtain. As can be seen from Figure 12, compared with condition 5, condition 8 smoke accelerates to the atrium, and condition 9 only a small amount of smoke can spread outward through the wind wall. The 15° wind screen installation angle has a greater perturbation on the smoke in the small compartment, so that the smoke spreads to the outside almost in the form of a jet stream. The different angles of the wind screen are ranked according to the excellent effect as follows: condition 9>condition 5>condition 8>condition 10.

(a) Left view of the flue gas diffusion distribution at 20s, from left to right, condition 5, 8, 9 and 10 in order.

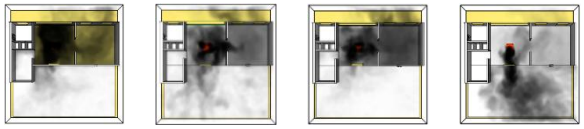

(b) Top view of the smoke dispersion distribution at 50s, from left to right for conditions 5, 8, 9 and 10.

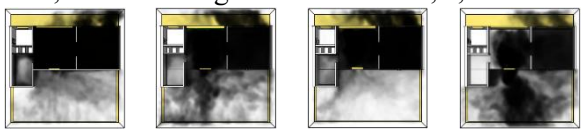

(c) Top view of smoke spread distribution at 90s, from left to right for conditions 5, 8, 9 and 10

Figure 12. Flue Gas Spread

5.3.2 Smoke blocking efficiency

From Figure 13, we can get the order of smoke blocking efficiency at each place according to the size: The order of smoke blocking efficiency at the door is as follows: condition 7>condition 9>condition 8>condition 10. The order of smoke blocking efficiency at the left window is as follows: condition 10>condition 8>condition 9>condition 7. The order of smoke blocking efficiency at the right window is as follows: condition 10>condition 8>condition 9>condition 7.

The installation angle of the air curtain has a greater impact on the heat flux at the exit, increasing the inclination angle of the air curtain will reduce the smoke blocking efficiency of the air curtain at the doorway, but increase the smoke blocking efficiency of the air curtain at the window. Air curtain inclination angle of 15 ° on the smoke blocking efficiency of the great influence, in the luxury cruise ship cabin fire design basically do not need to consider more than 15°.

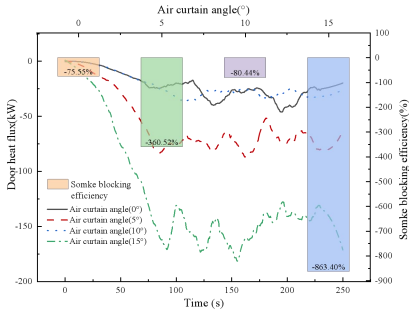

(a) Door heat flux and smoke blocking efficiency graphs

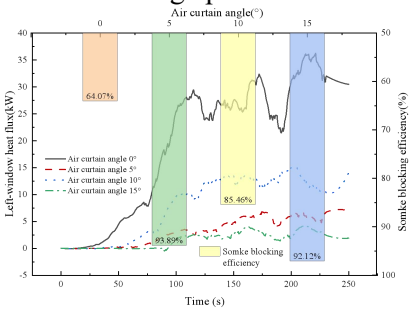

(b) Heat flux and smoke blocking efficiency of the left window

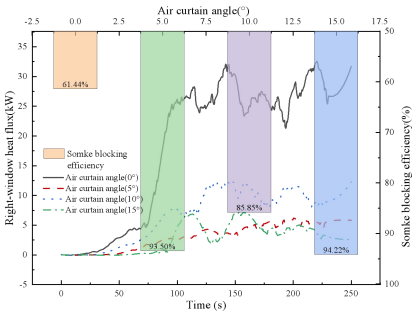

(c) Heat flux and smoke blocking efficiency of the right window

Figure 13. Heat Circulation and Smoke Barrier Efficiency of Doors and Windows with Different Air Curtain Wind Speeds

6. Conclusion

This study employs a composite material of nano-silica and zinc borate to construct an air curtain generator, which demonstrates three significant advantages: Firstly, its porous structure effectively blocks over 90% of thermal radiation. Secondly, the silicon-phosphorus cross-linked char layer maintains structural stability under high-temperature conditions. Thirdly, the water-based slurry spraying technology proves suitable for installation on curved ship surfaces. Experimental verification shows that when subjected to direct flame impact at 700°C, the outlet temperature of the composite-based air curtain rises merely to 120°C—significantly lower than the 450°C observed in traditional aluminum alloy materials—effectively overcoming the insufficient fire resistance of conventional fire protection equipment in high-temperature environments.

Comprehensive analysis indicates that the marine fire-smoke curtain developed in this study, as an innovative firefighting measure, exhibits exceptional thermal insulation and smoke-blocking efficacy during ship fires. Characterized by its non-water-based composition, low intervention, and intelligent responsiveness, this fire-smoke curtain system overcomes the limitations of traditional sprinkler systems in large-volume spaces, providing an innovative solution for whole-life-cycle fire protection aboard vessels. Simultaneously, this technology offers a replicable technical paradigm for industrial safety applications, serving as a crucial supplement to smoke control designs in large-volume spaces of luxury cruise ships, thus strengthening the safeguarding of maritime fire safety.

Acknowledgments

National Natural Science Foundation of China (71103122).

References

[1] Ren Yanluo and Zhu Shiwei. Research on the Development Situation of China's Cruise Tourism Industry. Commercial Culture, 2020, (27):90-91.

[2] JIA Jia, LU Shouxiang. Research on fire risk analysis method of ship compartment. Journal of Safety and Environment,2014,14(3):132-137.

[3] HUANG Dongmei. Numerical simulation study on smoke prevention effect of single blowing smoke-proof air curtain. Southwest Jiaotong University, 2008.

[4] F. C. Hayes， W. F. Stoecker. Heat Transfer Characteris tics of the Air Curtain, ASHRAE Transactions, Vol.75, Part11,1969.

[5] Y. T Ge, S. A Tassou.Simulation of the performance of single jet air curtains for vertical refrigerated display cabinets. Applied Thermal Engineering,2011,21(2).

[6] Hu L. H, Zhou J. W., Huo R., et al. Confinement of fire-induced smoke and carbon monoxide transportation by air curtain in channels. Journal of Hazardous Materials,2008,156(1):327-334.Chun Mei Guo, Yan Li. The Effect of Air Curtain on Controlling Contaminants in Wards Scientific.2012,433:1265-1270.

[7] Yang Hua, Yuen R., Zhang Heping. Numerical Study of Smoke Control for Underground Platform in a High-Speed Railway Station. Applied Mechanics and Materials,2012.

[8] Chun Mei Guo, Yan Li. The Effect of Air Curtain on Controlling Contaminants in Wards Scientific.2012,433:1265-1270.

[9] Goncalves, JC, Costa, JJ, Figueiredo, AR, Lopes, AMG.CFD modelling of aerodynamic sealing by vertical and horizontal air curtains, ENERGY AND BUILDINGS,2012,52:153-160.

[10] Tomas Gil-Lopez, Juan Castejon-Navas, Miguel A. Galvez-Huerta, Paul G. O'Donohoe. Energetic, en vironmental and economic analysis of climatic sep aration by means of air curtains in cold storage rooms,2014(74):8-16 ZHONG Chenhua, ZHU Xiaojun, LIU Kai, et al. Application of Vortex Sequencing of Air Jet Streams to Smoke Barriers. China Journal of Safety Science,2013,23(5):33-37.

[11] ZHONG Chenhua, ZHU Xiaojun, YANG Zhiqing, et al. Smoke barrier method for air vortex plugs in ship channels based on air vortex structural characteristics. Journal of Naval Engineering University,2013,25(4):74-78.

[12] Zhong Chenhua, Zhu Xiaojun, Yang Zhiqing et al. Air vortex plug smoke barrier method for ship channels based on air vortex structure characteristics. Journal of Naval University of China, 2013,25(4):74-78.

[13] Luo Na, Li Angui, Leng Bin, et al. Smoke Confinement with Multi-Stream Air Curtain at Stairwell Entrance. Procedia Engineering,2017,205:337-344.

[14] Zhang Xiaotao, Tan Chong, Lu Yu. Numerical Analysis of Smoke Confinement by Means of Air Curtains in High-Rise Buildings.

Applied Mechanics and Materials,2016.
[15] Razeghi S, Safarzadeh M, Pasdarshahri H. Evaluation of air curtain and emergency exhaust system for smoke confinement of an enclosure. Journal of Building Engineering,2020,33:101650.
[16] Tianhong Zhang, Rubing Han, Numerical study on the influence of subway platform air curtains on smoke diffusion, Case Studies in Thermal Engineering, Volume 2023,50.
[17] Longxing Yu, Yinnan Chen, Shuo Chen, Yuxuan Zhang, Hao Zhang, Chunxiang Liu, Numerical analysis of the performance of a PID-controlled air curtain for fire-induced smoke confinement in a tunnel configuration, Fire Safety Journal, Volume 2023,141.
[18] Tao Li, Zhengquan Chen, Wenxuan Zhao, Jianing Yuan, Chunxiang Wang, Yuchun Zhang, Study on the smoke sealing efficiency of air curtain and maximum ceiling temperature rise under longitudinal ventilation in bifurcated tunnel, International Journal of Heat and Fluid Flow, 2025,112
[19] Xinling Lu, Miaocheng Weng, Fang Liu, Junjie Yu, Study on smoke sealing effectiveness of the air curtain in exit bifurcated tunnel fires, Case Studies in Thermal Engineering, 2024,63.
[20] Paulo César França da Câmara, Stéphanie Cavalcante de Morais, Nívia do Nascimento Marques, Elessandre Alves de Souza, Rosangela de Carvalho Balaban, Cellulose nanocrystals reinforcement for glycerol-based gels: Effects on gelation behavior and thermal insulation performance, Journal of Molecular Liquids, 2025,428.
[21] SHI Huiming, FANG Shengrong, WANG Hongjiao. Research on the influence law of air curtain on fire smoke in train compartment. Fire Science and Technology,2021,40(04):467-470.
[22] Shi Hongwei et al., Nanoscale SiO_2/Modified Acrylic Resin Low-Surface-Energy Anti-Fouling Coatings. Journal of Materials Progress, 2014.1.
[23] Gao Shun et al. Synergistic flame retardant mechanism of nano-SiO2 and RDP on PC-ABS alloy. Journal of Composite Materials, 2020.1.
[24] Liang Zhiyuan. The influence of smoke-proof air curtain and mechanical smoke exhaust combined effect on smoke gas control in ship's cabin area. University of Science and Technology of China, 2021.
[25] HE Xuechao, WANG Jingwei, ZHANG Wenhua, et al. Investigation and confidence analysis of fire loads in clothing stores indifferent cities_He Xuechao. Fire Science and Technology,2012,31(11):1219-1221.
[26] Cheng Chao. Research on fire simulation modeling and safety of large shopping mall fire based on fire load. Nanhua University,2019.

